

OPEN CHARM PRODUCTION AND SPECTROSCOPY AT LHCb

Patrick Spradlin
on behalf of the LHCb collaboration

University of Glasgow Particle Physics

VIII International Workshop on Charm Physics (Charm 2016)
05-09 September 2016
Bologna, Italy



OUTLINE

1 INTRODUCTION

- LHCb
- Real-time alignment and calibration and Turbo stream

2 PRODUCTION MEASUREMENTS

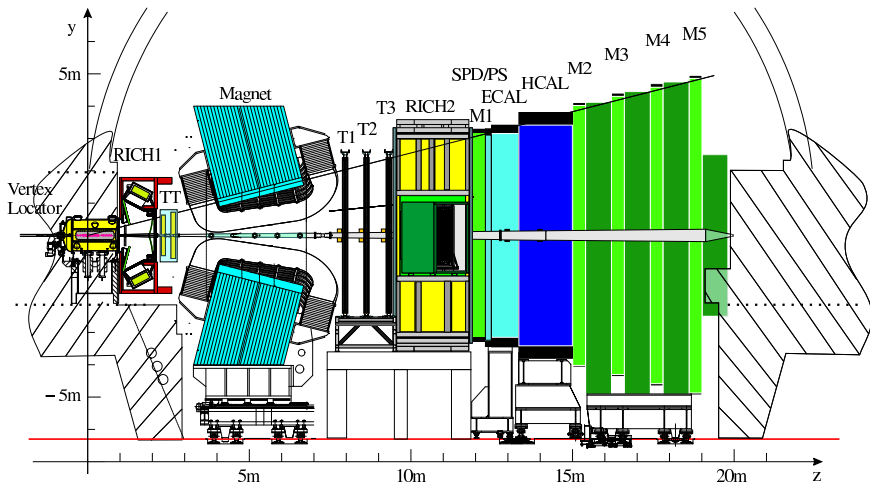
- Introduction and impact
- 13 TeV charm meson cross-sections ([JHEP 1603 \(2016\) 159](#))
- 5 TeV charm cross-sections (LHCb-PAPER-2016-042, **New!**)
See *presentation by D. Müller on Wednesday*.
- D^0 production in p -Pb ([LHCb-CONF-2016-003](#))
- $\Upsilon + D$ associated production ([JHEP 1607 \(2016\) 052](#))

3 SPECTROSCOPY MEASUREMENTS

- Introduction
- Inclusive $D^{*+}\pi^-$ ([JHEP 1309 145](#))
- Dalitz analysis of $B^- \rightarrow D^+\pi^-\pi^-$ ([arXiv:1608.01289](#))

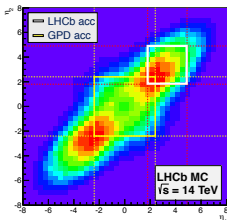
LHCb DETECTOR

LHCb: a single-arm forward spectrometer at the LHC.

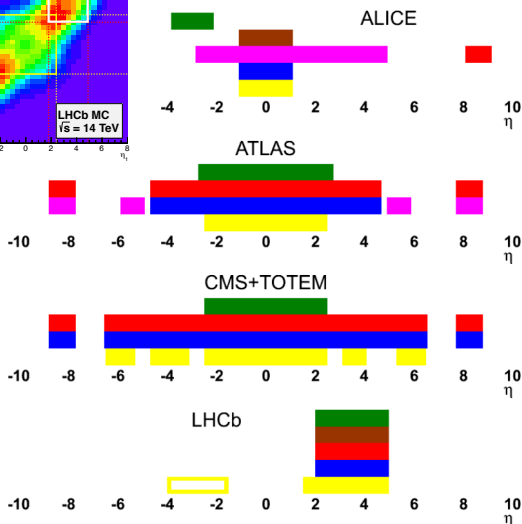


Optimized for heavy flavor physics in pp collisions.

LHCb ACCEPTANCE



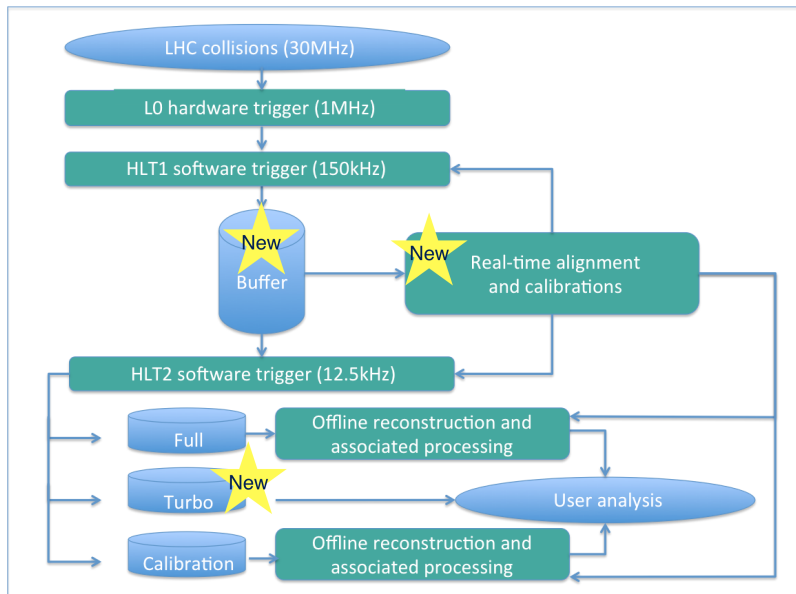
Pseudorapidity of b and \bar{b} produced in pp collisions for LHCb simulation.



- ALICE
 - central
 - forward muon coverage
- ATLAS & CMS
 - central detectors
- LHCb
 - forward detector
 - tracking, particle-ID and calorimetry in full acceptance

- hadron PID
- muon system
- lumi counters
- HCAL
- ECAL
- tracking

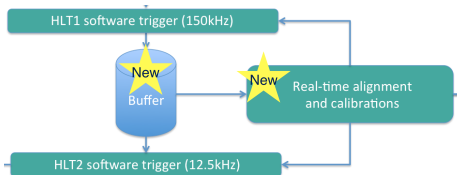
LHCb RUN 2 DATAFLOW



REAL-TIME CALIBRATION & TURBO STREAM

It is a matter of precision!

- Increased cross-sections and bunch-crossing rate \Rightarrow event rate increase,
- HLT software trigger must be more selective than it was in Run 1,
- In order to meet LHCb's need for precision, the event reconstruction in HLT2 must be as precise as offline reconstruction,
- **The detector calibration must be done prior to HLT2.**



Buffering also allows continuous use of farm throughout inter-fill.

Since the HLT2 reconstruction is offline-quality, use it in analysis directly!

In the Turbo stream, keep all information necessary for analysis,

- Particle and decay candidates as reconstructed in Hlt2,
- Additional information for specific measurements.

More data and greater physics reach for the same computing resources!

HEAVY FLAVOR PRODUCTION

Production measurements of heavy flavor hadrons can be vital to improved understanding of QCD,

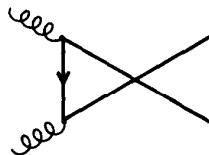
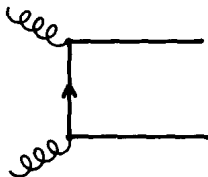
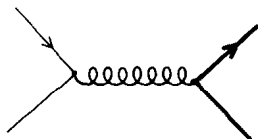
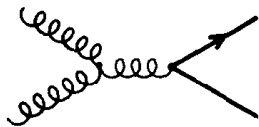
- Test precise cross-section predictions,
- Provide empirical fragmentation functions,
- Probe proton structure at low x .

Necessary for MC generator tuning,

- Simulation inputs to precision flavor physics measurements,
- Long term program planning,
- New experiment design.

Standard Model backgrounds for New Physics searches,

- Absolute rates of SM processes must be known precisely.



HEAVY PRODUCTION AND PROTON STRUCTURE

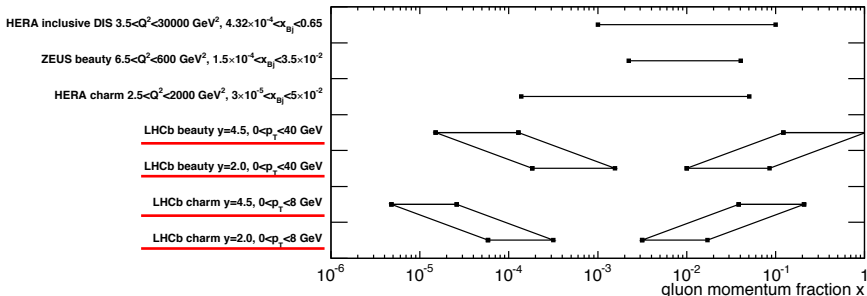
Heavy flavor forward production in LHC proton-proton collisions primarily through **gluon-gluon fusion**.

LHCb flavor production measurements cover a partonic momentum fraction x complementary to the HERA DIS data,

- HERA: $10^{-4} < x \lesssim 10^{-1}$,
- LHCb: $5 \times 10^{-6} < x \lesssim 10^{-4}$.

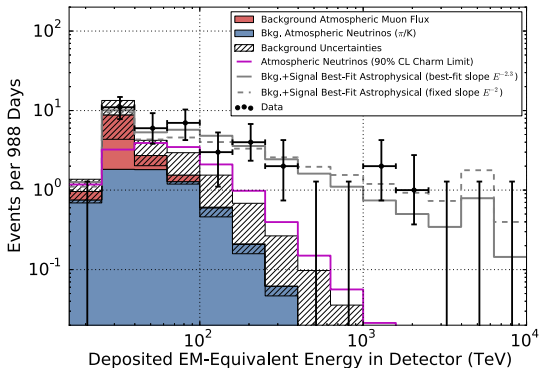
Inclusion of LHCb data should improve precision of gluon PDFs at small x ,

- Implications for lepton flux calculations in atmospheric showers.



CHARM AND ASTROPHYSICAL NEUTRINOS

Atmospheric charm production and decay is a dominant source of background for ultra-high-energy neutrino astrophysics.



IceCube, PRL 113 (2014) 101101.

Energy of IceCube observed events with predictions of atmospheric sources and overall fit.



NEUTRINOS FROM ATMOSPHERIC CHARM

LHC measurements relevant to neutrinos from atmospheric charm production,

- pp at $\sqrt{s} = 7$ TeV (13 TeV) corresponds to incoming cosmic ray of $E = 26$ PeV (90 PeV).

Gauld *et al.* performed a PDF improvement similar to PROSA,

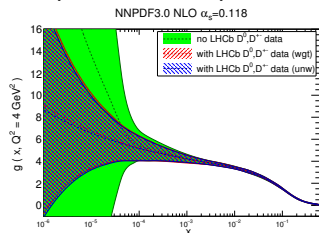
- NNPDF3.0 NLO set reweighted to match LHCb charm cross-sections at 7 TeV.

Significant improvement in precision at small x .

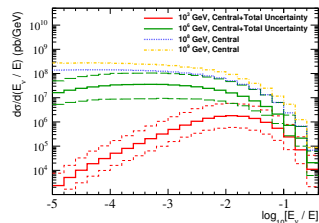
Improved PDF set used in POWHEG and other MC generators,

- Charm production cross-sections in LHC $\sqrt{s} = 13$ TeV collisions,
- Atmospheric charm production in high-energy cosmic ray interactions.

See also Bhattacharya *et al.*, [JHEP 06 \(2015\) 110](#).



NNPDF3.0 NLO small- x gluon with LHCb charm



Differential cross-section of charm-induced neutrino production.

DIFFERENTIAL CROSS-SECTIONS

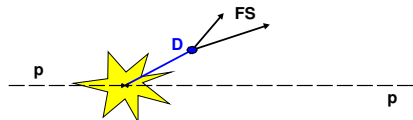
Differential production cross-sections of D mesons (H_C),

$$\frac{d^2\sigma_i(H_C)}{dp_T dy} = \frac{1}{\Delta p_T \Delta y} \cdot \frac{N_i(H_C \rightarrow f + \text{c.c.})}{\varepsilon_{i,\text{tot}}(H_C \rightarrow f) \cdot \mathcal{B}(H_C \rightarrow f) \cdot \mathcal{L}_{\text{int}}}$$

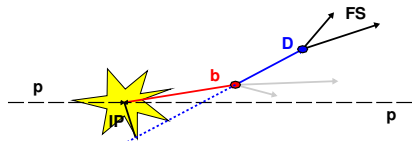
in bins of p_T and y with respect to the collision axis.

- $N_i(H_C \rightarrow f + \text{c.c.})$: signal yield in bin i ,
- $\varepsilon_{i,\text{tot}}(H_C \rightarrow f)$: total signal efficiency
 - Factorized into components, *e.g.*, track reconstruction efficiency, PID efficiency, selection efficiency, *etc.*
 - Components evaluated in independent data samples where possible,
 - Estimated from simulation when not possible.
- \mathcal{L}_{int} : integrated luminosity of sample,

CHARM IN HADRONIC COLLISIONS



Prompt production



b decays ($B \rightarrow D^{(*)} X$)

Two major sources of charm:

- Prompt: Produced at primary interaction,
 - Direct production,
 - Feed-down from higher resonances.
- Secondary: Produced in the decay of a b -hadron.

Separate the prompt and secondary components,

- Secondary treated as background for D meson cross-sections.

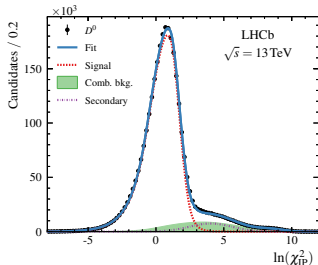
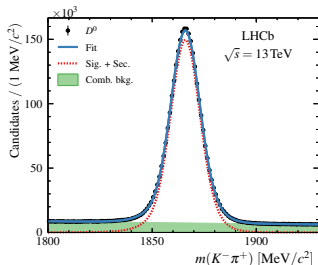
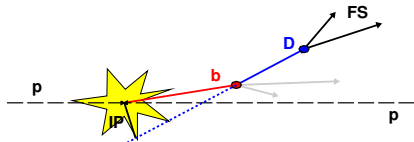
D^0 , D^+ , D_s^+ , AND D^{*+} CROSS-SECTIONS

D meson cross-sections now measured at three pp collision energies

- $\sqrt{s} = 7$ TeV: $\mathcal{L}_{\text{int}} = 15 \text{ nb}^{-1}$
Nucl.Phys. B871 (2013) 1-20,
- $\sqrt{s} = 13$ TeV: $\mathcal{L}_{\text{int}} = 5 \text{ pb}^{-1}$
JHEP 1603 (2016) 159,
- $\sqrt{s} = 5$ TeV: $\mathcal{L}_{\text{int}} = 9 \text{ pb}^{-1}$
LHCb-PAPER-2016-042 (New).

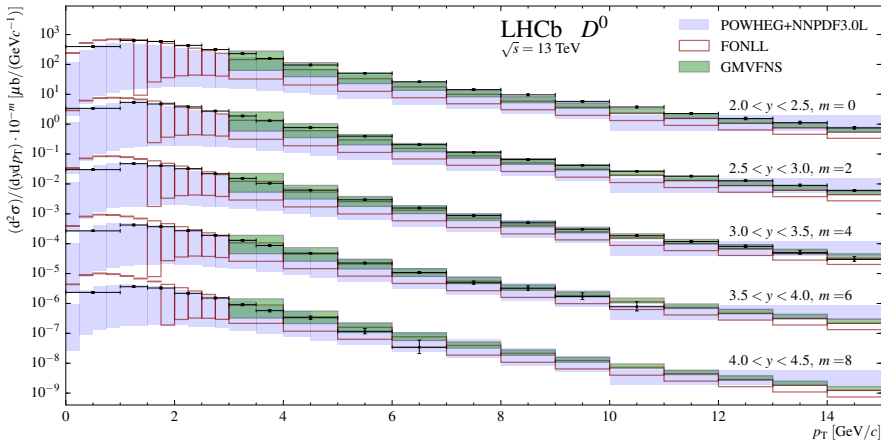
13 TeV and 5 TeV: Analysis of HLT2 candidates with Turbo stream.

Separation of prompt and secondary charm with $\log(IP\chi^2)$ distribution,



D⁰ production at $\sqrt{s} = 13$ TeV (JHEP 1603 (2016) 159)

PROMPT D^0 CROSS-SECTIONS AT $\sqrt{s} = 13$ TeV



FONLL: Cacciari et al., [Eur.Phys.J. C75 \(2015\) 610](#),
 POWHEG+NNPDF3.0L: Gauld et al., [JHEP 1511 \(2015\) 009](#),
 GMVFS: Kniehl et al., [Eur.Phys.J. C72 \(2012\) 2082](#).

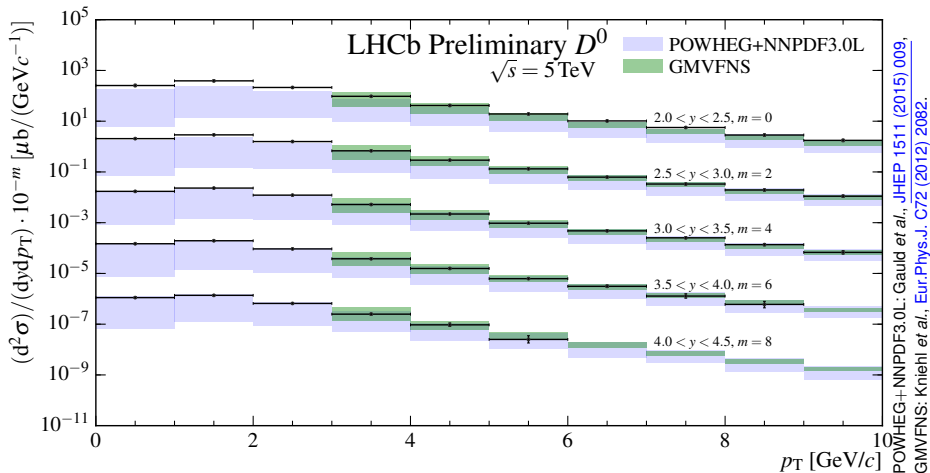
Double differential cross-sections, $d^2\sigma_i/dp_T dy$, of prompt D^0 vs. p_T .

Integrated over the acceptance of the analysis

$$\sigma(D^0, p_T < 8 \text{ GeV}, 2.0 < y < 4.5) = 3240 \pm 4 \pm 190 \mu\text{b}.$$



PROMPT D^0 CROSS-SECTIONS AT $\sqrt{s} = 5 \text{ TeV}$

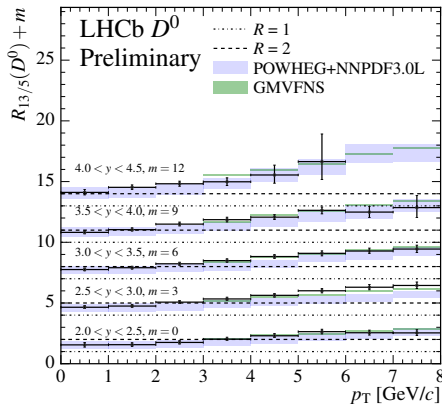
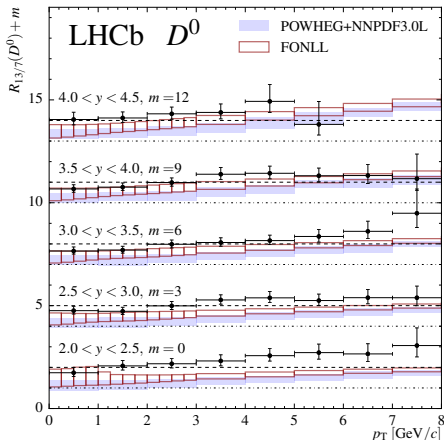


Double differential cross-sections, $d^2\sigma_i/dp_T dy$, of prompt D^0 vs. p_T .

Integrated over the acceptance of the analysis

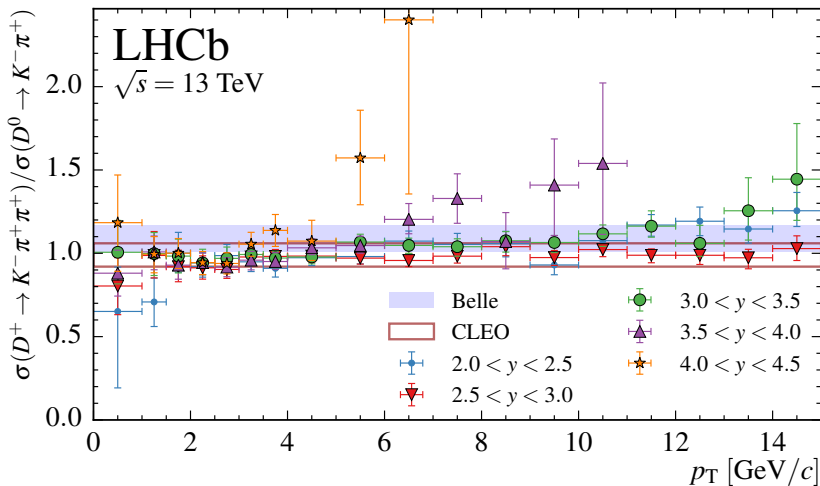
$$\sigma(D^0, p_T < 8 \text{ GeV}, 2.0 < y < 4.5) = 1635 \pm 4 \pm 89 \mu\text{b}.$$

COMPARISONS: 13 TeV RELATIVE TO 7 TeV AND 5 TeV



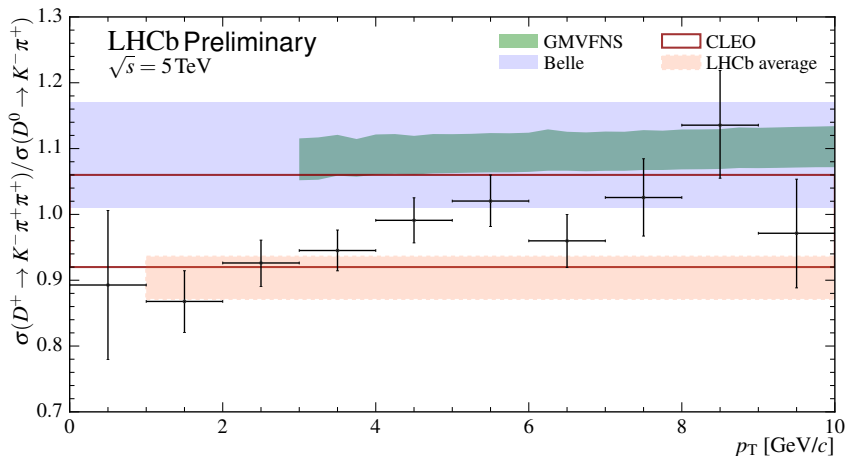
Ratios of double differential cross-sections, $d^2\sigma_i/dp_T dy$, between measurements at $\sqrt{s} = 13$ TeV and at $\sqrt{s} = 7$ TeV (left) and $\sqrt{s} = 5$ TeV (right).

For each interval, the dash-dotted line represents a ratio of 1.

RATIOS AT 13 TeV: D^+ / D^0 

Ratios of double differential cross-sections, $d^2\sigma_i/dp_T dy$, between D^+ and D^0 measurements at $\sqrt{s} = 13 \text{ TeV}$.

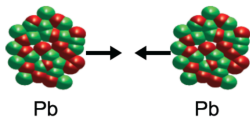


RATIOS AT 5 TeV: D^+ / D^0 

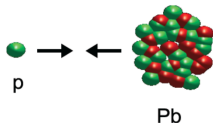
Ratios of differential cross-sections, $d\sigma_i/dp_T$ integrated over $2 < y < 4.5$, between D^+ and D^0 measurements at $\sqrt{s} = 5 \text{ TeV}$.

D^0 PRODUCTION IN p -Pb COLLISIONS

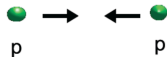
Heavy flavor production can be used to study the properties of quark-gluon plasma in nucleus-nucleus collisions



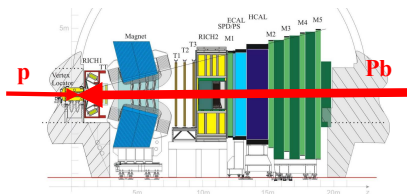
However, the cold nuclear matter effects must be disentangled from plasma effects. These can be studied in nucleon-nucleus (p -Pb) collisions



The study of cold nuclear matter effects relies on nucleon-nucleon interactions (p - p) as a reference.

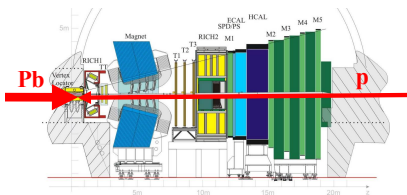


LHCb collected p -Pb data at mean nucleon-nucleon collision energy $\sqrt{s_{NN}} = 5$ TeV.



p on Pb collisions (forward)

$$\mathcal{L}_{\text{int}} \sim 1.1 \text{ nb}^{-1}, \quad 1.5 < y^*(D) < 4.0.$$



Pb on p collisions (backward)

$$\mathcal{L}_{\text{int}} \sim 0.5 \text{ nb}^{-1}, \quad -5.0 < y^*(D) < -2.5.$$

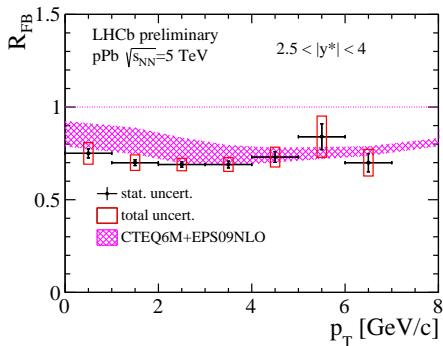
D^0 CROSS-SECTIONS IN p -Pb

Double-differential D^0 production cross-sections in p -Pb, $d^2\sigma/dy^*dp_T$,

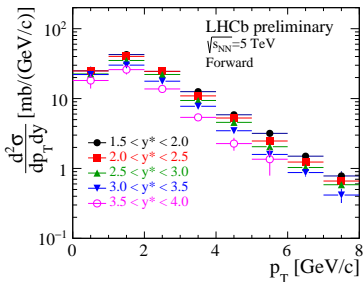
- y^* and p_T in the nucleon-nucleon CoM,
- Measured wrt. the p momentum direction.

Forward-backward cross-section asymmetry:

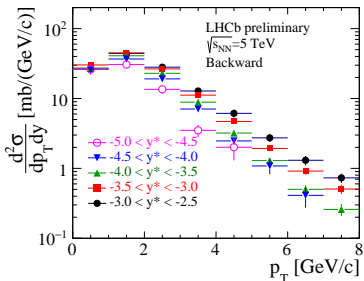
$$R_{FB}(y^*, p_T; \sqrt{s_{NN}}) \equiv \frac{\sigma_{pPb}(+|y^*|, p_T; \sqrt{s_{NN}})}{\sigma_{pPb}(-|y^*|, p_T; \sqrt{s_{NN}})}$$



Forward ($p \rightarrow Pb$)



Backward ($Pb \rightarrow p$)



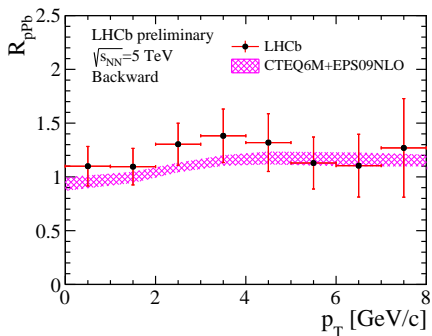
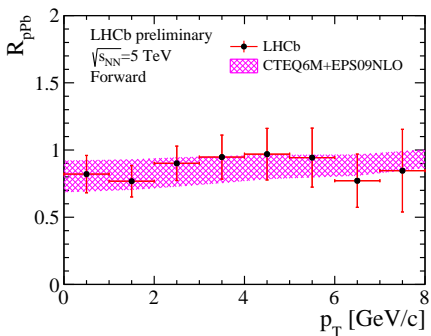
NUCLEAR MODIFICATION FACTOR

Effects of cold nuclear medium expressed relative p - p cross-sections:

$$R_{pPb}(y^*, p_T; \sqrt{s_{NN}}) \equiv \frac{1}{A} \frac{d^2\sigma_{pPb}(y^*, p_T; \sqrt{s_{NN}})/dy^* dp_T}{d^2\sigma_{pp}(y^*, p_T; \sqrt{s_{NN}})/dy^* dp_T}, A = 208$$

This preliminary result determined before the 5 TeV p - p cross-section,

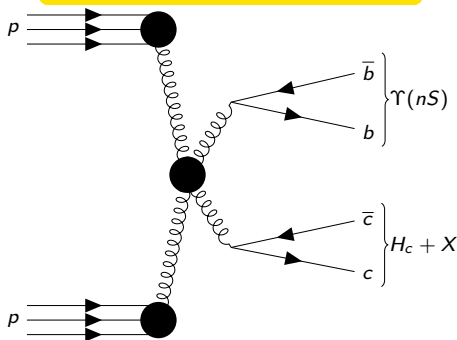
- σ_{pp} estimated by extrapolation from the 7 TeV and 13 TeV cross-sections,
- Update in progress.



CTEQ6M+EPS09NLO: Mangano *et al.*,
Nucl.Phys. B373 (1992) 295-345.

MULTIPLE HEAVY QUARK PRODUCTION

Single Parton Scattering (SPS)

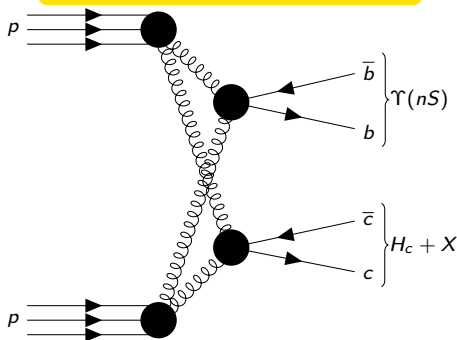


Both heavy flavor pairs from a single hard parton-parton interaction.

NRQCD: (Berezhnoy and Likhoded, [JMPA 30 1550125](#))

$$R_{\text{SPS}} \equiv \frac{\sigma^{\Upsilon c\bar{c}}}{\sigma^{\Upsilon}} = (0.2 - 0.6)\%.$$

Double Parton Scattering (DPS)



Two independent parton collisions.

$$\sigma^{\Upsilon c\bar{c}} = \frac{\sigma^{\Upsilon} \times \sigma^{c\bar{c}}}{\sigma_{\text{eff}}}$$

$$R_{\text{DPS}} \equiv \frac{\sigma^{\Upsilon c\bar{c}}}{\sigma^{\Upsilon}} = \frac{\sigma^{c\bar{c}}}{\sigma_{\text{eff}}} \approx 10\%.$$

$\Upsilon + D$ ASSOCIATED PRODUCTION

LHCb Run 1 data

- 1 fb^{-1} of pp at $\sqrt{s} = 7 \text{ TeV}$,
- 2 fb^{-1} of pp at $\sqrt{s} = 8 \text{ TeV}$.

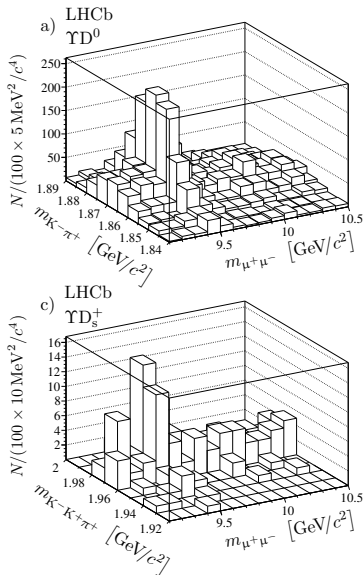
Coincidences of $b\bar{b}$ states and open charm,

- $\Upsilon(nS) \rightarrow \mu^+ \mu^-$ for $n = 1, 2, 3$,
- D^0, D^+, D_s^+ , and Λ_c^+ in decays to CF hadronic modes.

First observations in excess of 5σ significance for 5 combinations,

- $\Upsilon(1S)+D^0, \Upsilon(1S)+D^+, \Upsilon(1S)+D_s^+,$
 $\Upsilon(2S)+D^0,$ and $\Upsilon(2S)+D^+.$

Measured cross-sections and differential distributions of kinematic variables.



$\Upsilon + D$ VIA DPS

Measured cross-sections

$$\sigma_{\sqrt{s}=7\text{ TeV}}^{\Upsilon(1S)D^0} \times \mathcal{B}(\Upsilon(1S) \rightarrow \mu^+ \mu^-) = 155 \pm 21 \pm 7 \text{ pb},$$

$$\sigma_{\sqrt{s}=7\text{ TeV}}^{\Upsilon(1S)D^+} \times \mathcal{B}(\Upsilon(1S) \rightarrow \mu^+ \mu^-) = 82 \pm 19 \pm 5 \text{ pb}.$$

From which are computed

$$R_{\sqrt{s}=7\text{ TeV}} \frac{\sigma^{\Upsilon(1S)c\bar{c}}}{\sigma^{\Upsilon(1S)}} \Big|_{\sqrt{s}=7\text{ TeV}} = (7.7 \pm 1.0)\%.$$

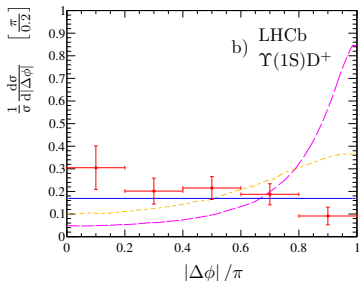
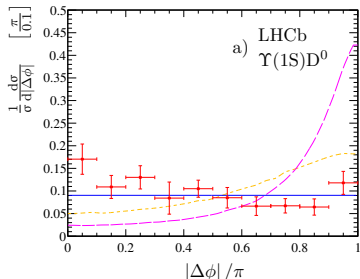
Significantly larger than theoretical predictions.

Azimuthal angle, $\Delta\phi$, between Υ and D

- Flat, consistent with independent,
- Production dominated by DPS.

Computations of normalization factor σ_{eff} assuming DPS,

$\sigma_{\text{eff}}|_{\Upsilon(1S)D^0} = 19.4 \pm 2.6 \pm 1.3 \text{ mb}$
 consistent with values from previous measurements in other channels



Orange and magenta dashed lines: predictions of SPS.

SPECTROSCOPY MEASUREMENTS AT LHCb

INCLUSIVE STUDIES OF $H_c + h$

$$pp \rightarrow (D\pi)_{D_J} X, \quad pp \rightarrow (DK)_{D_{sJ}} X$$

- All resonances are accessible,
- Large backgrounds,
- Spin-parity analysis only applicable to three-body decays,
 - Only distinguishes between natural and unnatural parity.

$$D^+ \pi^-, D^0 \pi^+, D^{*+} \pi^-: \text{JHEP 1309 145}$$

$$D^+ K_s^0, D^0 K^+: \text{JHEP 1210 151}$$

AMPLITUDE ANALYSIS b -HADRON DECAYS TO CHARMED HADRONS

- Full spin-parity analysis,
- Limited access to high-mass resonances,
- Complicated analysis of multiple interfering states.

$$B^- \rightarrow D^+ \pi^- \pi^-: \text{arXiv:1608.01289}$$

$$B^- \rightarrow D^+ K^- \pi^-: \text{PRD 91 092002, PRD 93 119901}$$

$$B^0 \rightarrow \bar{D}^0 \pi^+ \pi^-: \text{PRD 92 032002}$$

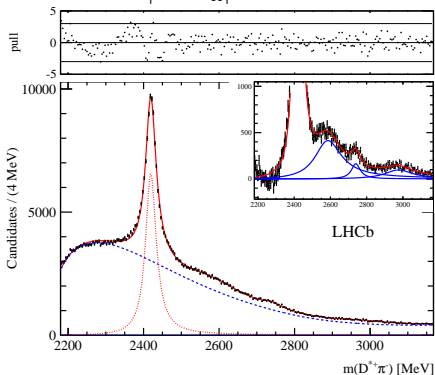
$$B^0 \rightarrow \bar{D}^0 K^+ \pi^-: \text{PRD 92 012012}$$

$$B_s^0 \rightarrow \bar{D}^0 K^- \pi^+: \text{PRL 113 162001, PRD 90 072003}$$

MASS FITS FOR $D^{*+}\pi^{-}$

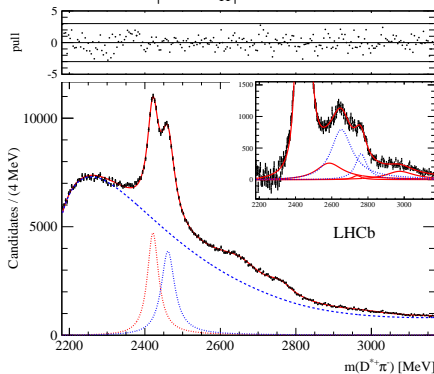
Enhanced unnatural parity

$$|\cos\theta_H| > 0.75$$

Dominated by $D_1(2420)^0$.Three additional structures observed
 $D_J(2580)^0$, $D_J(2740)^0$, $D_J(3000)^0$.

Natural parity subsample

$$|\cos\theta_H| < 0.5$$

Large $D_1(2420)^0$ and $D_2^*(2460)^0$ features. $D_J(2580)^0$, $D_J(2740)^0$, and $D_J(3000)^0$, fixedTwo additional structures observed
 $D_J^*(2650)^0$, $D_J^*(2760)^0$.

ANGULAR ANALYSIS OF $D^{*+}\pi^{-}$

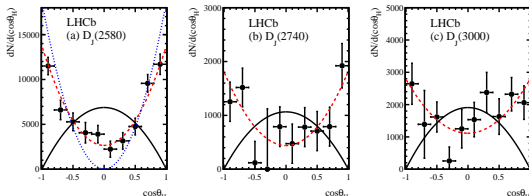
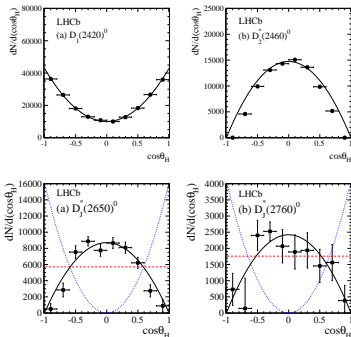
Data set partitioned in to 10 slices of helicity angle.

Yields of each structure determined as a function of $\cos\theta_H$.

$D_1(2420)^0$ and $D_2^*(2460)^0$ consistent with expected $J^P = 1^+$ and 2^+ respectively.

$D_J^*(2650)^0$ and $D_J^*(2760)^0$ consistent with having natural parity.

Angular distributions for $D_J(2580)^0$, $D_J(2740)^0$, and $D_J(3000)^0$ are consistent with having unnatural parity.

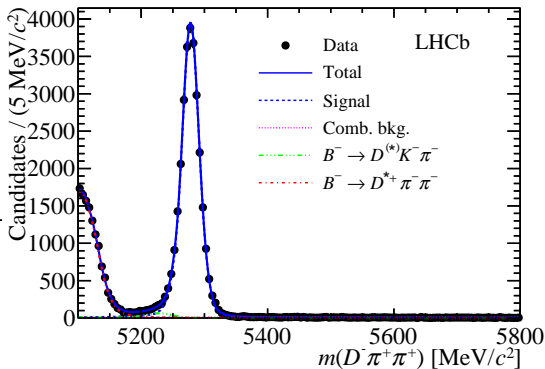
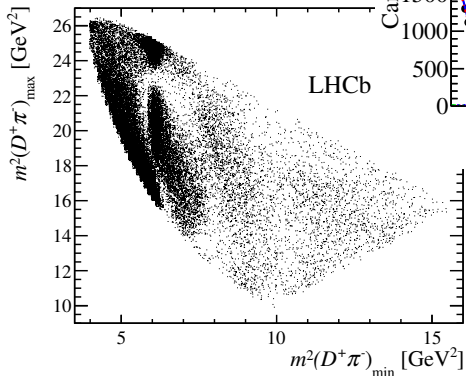


DALITZ ANALYSIS OF $B^- \rightarrow D^+ \pi^- \pi^-$

Dalitz analysis of $27\,956 \pm 195$
 $B^- \rightarrow D^+ \pi^- \pi^-$ decays

● Signal purity $\sim 98.5\%$

Full 3 fb^{-1} of LHCb Run 1 data.



Identical pions ordered by
 magnitude of $m^2(D^+ \pi^-)$
 $m^2(D^+ \pi^-)_{\min}, m^2(D^+ \pi^-)_{\max}$

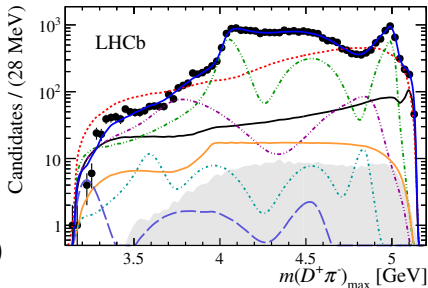
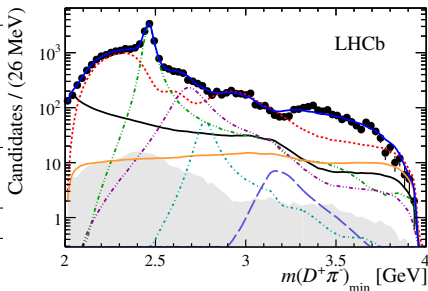
DALITZ ANALYSIS OF $B^- \rightarrow D^+ \pi^- \pi^-$

Resonance	Fit fraction (%)
$D_2^*(2460)^0$	$35.69 \pm 0.62 \pm 1.37 \pm 0.89$
$D_1^*(2680)^0$	$8.32 \pm 0.62 \pm 0.69 \pm 1.79$
$D_3^*(2760)^0$	$1.01 \pm 0.13 \pm 0.13 \pm 0.25$
$D_2^*(3000)^0$	$0.23 \pm 0.07 \pm 0.07 \pm 0.08$
$D_v^*(2007)^0$	$10.79 \pm 0.68 \pm 0.74 \pm 2.34$
B_v^*	$2.69 \pm 1.01 \pm 1.43 \pm 1.61$
Total S-wave	$56.96 \pm 0.78 \pm 0.62 \pm 0.87$

Resonance parameters (MeV)	
$D_2^*(2460)^0$	$m = 2463.7 \pm 0.4 \pm 0.4 \pm 0.6$ $\Gamma = 47.0 \pm 0.8 \pm 0.9 \pm 0.3$
$D_1^*(2680)^0$	$m = 2681.1 \pm 5.6 \pm 4.9 \pm 13.1$ $\Gamma = 186.7 \pm 8.5 \pm 8.6 \pm 8.2$
$D_3^*(2760)^0$	$m = 2775.5 \pm 4.5 \pm 4.5 \pm 4.7$ $\Gamma = 95.3 \pm 9.6 \pm 7.9 \pm 33.1$
$D_2^*(3000)^0$	$m = 3214 \pm 29 \pm 33 \pm 36$ $\Gamma = 186 \pm 38 \pm 34 \pm 63$

First observations of $D_3^*(2760)^0$, $D_2^*(3000)^0$

- Parameters of $D_3^*(2760)^0$ with $D_j^*(2760)$ observed in inclusive analysis.



SUMMARY

LHCb's forward design allows it to probe a unique region of heavy flavor production at LHC.

Heavy flavor production measurements with broad applications

- Tests of QCD calculations methods,
- Refinements of proton PDFs,
 - ⇒ Improved understanding of backgrounds for cosmic neutrino studies.
- Cold nuclear matter effects for quark gluon plasma studies,
- Examinations of double parton scattering.

Discovery and characterization of new states,

- Inclusive studies based on huge charm samples,
- Amplitude analyses of large samples of $b \rightarrow c$ decays.